

Investigation of the Operating Characteristics of a High-Power Hall Effect Thruster

Boris Arhipov,* Leonid Krochak,* and Nikolay Maslennikov†
Experimental Design Bureau "Fakel," 236001, Kaliningrad, Russia
and
Fabrizio Scortecci‡
CENTROSPAZIO, 56014 Pisa, Italy

An investigation aimed at evaluating the performance and operational characteristics of the SPT-200 was carried out by Fakel in collaboration with CENTROSPAZIO. The experimental characterization of the thruster was performed by measuring its electrical, propulsive, and operational parameters during a parametric test. Temperatures of the main thruster components were also measured in order to investigate the thruster thermal behavior. Tests were conducted at Fakel in a vacuum chamber of 17 m³ volume. The indicated background pressure, measured with ionization gauges calibrated for air, never exceeded 2.8×10^{-4} torr (uncorrected). The thruster was operated over a wide range of power levels, from 2 up to 12 kW. At the nominal operating point of 6 kW, the average specific impulse and efficiency, inclusive of all power losses and the cathode flow, were 1928 s and 0.59, respectively. The maximum efficiency of 0.63 was obtained at the 11 kW power level and 2950 s specific impulse.

Introduction

ELECTRIC propulsion has emerged in the last few years as a key technology enabling advanced mission and spacecraft concepts. In particular, the use of electric propulsion (EP) systems on board next-generation geostationary telecommunication satellites leads to very substantial savings in propellant mass. The potential applications encompass essentially all in-space satellite propulsion requirements. Use of EP for stationkeeping results in propellant mass savings of hundreds of kilograms. In the immediate future the increase of satellite power to 15–20 kW will allow EP systems to perform the transfer maneuver to geostationary orbit with additional savings of hundreds of kilograms of propellant. In the future EP systems will be used exclusively for all propulsion duties onboard telecom satellites. This tremendous saving of propellant mass will translate into a corresponding growth of satellite revenues, as it will be possible to increase greatly the number of transponders per satellite as well as the satellite operational lifetime and/or to reduce the launch cost by scaling down the selected launch vehicle.

Among the EP concepts developed to date, Hall effect thrusters with extended acceleration zone, also called stationary plasma thrusters (SPT), offer a great potential for future primary propulsion applications thanks to good performance and the possibility of scaling up the design for different power levels on the basis of well-demonstrated models and because of extensive flight heritage.^{1–3} However, implementing any new technology requires a thorough understanding not only of performance but also of integration issues. Electric propulsion is more challenging in this regard than chemical systems because of the difficulty in obtaining test results that are valid for on-orbit operations and because of concerns about the interactions that arise only with a fully deployed spacecraft. Therefore, to make a new thruster (especially of high power) attractive for commercial applications, extensive activity must be carried out to evaluate in detail its operational characteristics and its compatibility with other spacecraft subsystems.

An investigation aimed at evaluating the SPT 200 thruster produced by Fakel for propulsion applications at power levels up to

12 kW has been carried out by Fakel and CENTROSPAZIO with the collaboration of the Research Institute of Applied Mechanics and Electrodynamics of the Moscow Aviation Institute in the framework of a scientific collaboration sponsored by the International Association for the Promotion of Cooperation with Scientists from the New Independent States of the former Soviet Union (INTAS). The main objective of the collaboration was to investigate the thruster performance and operational characteristics, the thermal behavior, the plume characteristics, and the erosion of the discharge chamber. Some of these aspects were investigated experimentally by performing a parametric test on an existing engineering model thruster, whereas other aspects requiring an extensive testing activity or special very large facilities (i.e., for wear, plume, and thermal characteristics) were investigated theoretically.^{4–6}

Apparatus

Thruster

Substantial literature regarding the design and operational principles of SPT thrusters is available following research carried out in several laboratories.^{7–9} The SPT-200 thruster tested at Fakel was a model of classical design (i.e., the design characterizing the existing SPT-100 flight model) and did not feature any of the advanced configurations recently proposed on low-power models with the aim of optimizing some specific operational characteristics (high specific impulse, low plume divergence, lifetime). The thruster was an engineering model essentially new as it had undergone only a few hours of initial tests. It utilized four KE-50 cathode neutralizers to guarantee long-term operation during life testing (Fig. 1). The size of the thruster was about 26 × 26 × 20 cm, and the weight was about 12 kg. The KE-50 is also produced by Fakel and is capable of operating at up to 50 A. All testing was performed by using a single cathode; the remaining cathodes were not connected to the supply lines.

Vacuum Facility

Testing was conducted at Fakel in a vacuum chamber consisting of two sections: a cylindrical test section with a 2-m-diam × 2.3-m-long removable end cap and a 1.5-m-diam × 4-m-long manifold tube connecting the tank test section to the pumping system (Fig. 2). The overall internal volume is 17 m³.

The pumping system consists of five oil diffusion pumps backed by rotary pumps. Four diffusion pumps have a nominal pumping speed of 11,000 l/s each on air and are connected sideways to the vacuum chamber through 0.9-m-diam gate valves. One pump has

Received 1 March 1999; revision received 12 June 1999; accepted for publication 15 July 1999. Copyright © 1999 by the American Institute of Aeronautics and Astronautics, Inc. All rights reserved.

*Senior Scientist, Moskovsky prospekt 181.

†Senior Scientist, First Deputy Chief Designer, Moskovsky prospekt 181.

‡Senior Scientist, Manager, Via Gherardesca 5, Ospedaletto.

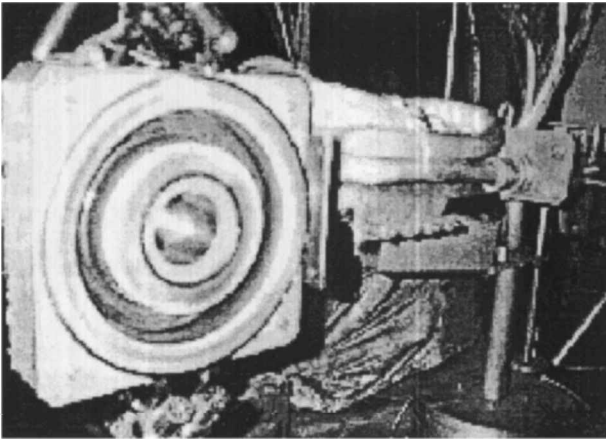


Fig. 1 SPT-200 thruster installed on the thrust stand.

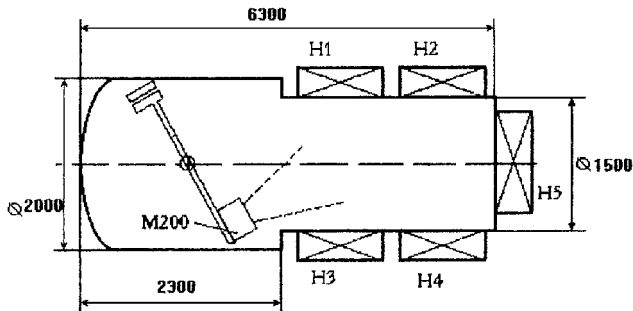


Fig. 2 Scheme of the vacuum facility test arrangement.

a nominal pumping speed of 13,000 l/s on air and is connected at one end of the manifold tube through a 1.2-m-diam gate valve. Thus, the total pumping speed of the system is about 57,000 l/s (for air).

The vacuum system provides an ultimate pressure of 7×10^{-6} torr and a dynamic pressure of 2.8×10^{-4} torr (uncorrected) at 20 mg/s xenon mass-flow rate, measured with ionization gauges calibrated for air (the correct background pressure value was obtained by dividing the reading by a 2.8 gas sensitivity factor). Therefore, the total pumping speed on Xenon is about 27,600 l/s.

Four ionization gauges were used to monitor the vacuum level along the axis of the manifold tube in the zone where the thruster exhausted its plume.

Propellant Feed System

The thruster did not include the integrated Xenon Flow Controller typical of flight models, and the feeding system was provided by a normal laboratory system.

Two feed lines, each consisting of a pressure regulator, a thermal flow meter, and a solenoid valve, were used to supply independently the anode and the active cathode. The propellant feedline pressure was dropped to the level required by the cathode and the anode within the respective pressure regulators located outside the vacuum chamber. Therefore, feedline pressure in the pipelines located between the pressure regulators and the feedthroughs of the chamber were lower than atmosphere, requiring one to check carefully for leaks to prevent contamination of the propellant. Thermal flow meters were calibrated in situ with a standard volumetric technique having an accuracy of $\pm 2\%$.

Xenon propellant with a purity grade in excess of 0.99996 was used during testing.

Power Supply System

The electric power system was provided by means of laboratory power supplies connected through a RLC matching network to the thruster. The main power supply consisted of a voltage regulated unit

having a 6% maximum ripple. Two power units were used to supply separately the internal and the external magnetizing coils. One unit was used to supply the cathode heater, while another independent unit was used to supply the cathode ignitor. A RLC matching network, designed on the basis of Fakel's past experience and consisting of a 16-mH inductor, a $15\text{-}\Omega$ resistor, and a $10\text{-}\mu\text{F}$ capacitor, was used to filter oscillations of the discharge circuit. Thruster electrodes were allowed to float.

Diagnostics and Instrumentation

Thrust was measured by means of a torsional balance of the type already described by Arhipov et al.¹⁰ The thrust stand was equipped with two separate calibration systems. A primary calibration system allowed the balance to be operated in a range of 0–500 mN with an uncertainty of $\pm 2.5\%$ of the full scale. A secondary calibration system, with a range of 0–200 mN was used to increase the operational range of the balance up to 700 mN. However, this second system showed a higher uncertainty ($\pm 5\%$ of its full scale), and therefore for measurements above 500 mN the total uncertainty of the balance increased up to $\pm 3.2\%$ of the total full scale. Data acquisition was performed manually by reading a number of analog devices. Voltages were measured by means of voltmeters having an accuracy of $\pm 1\%$. Currents were measured by measuring the voltage drop across a shunt. Discharge current oscillations were measured using a current transformer and a recording oscilloscope. Root-mean-square (rms) values of discharge current and voltage oscillations were measured by means of current/voltage transformer gauges and a recording oscilloscope. Flow rate, vacuum chamber pressure, and thrust were registered from the read out panels. Type K thermocouples were used to measure the thruster assembly temperatures.

A manual switch was used to temporarily ground the cathode for a few seconds to allow measurements of the ion current flowing from the thruster. This current was measured using an ammeter connected to the cathode-vacuum chamber housing circuit. The measurement was not continuously performed to prevent the discharge from extinguishing caused by cathode cool down.

Test Procedure

After placement of the thruster on the thrust stand of the test facility, the magnetic field was measured by means of a gaussmeter to check that the magnetizing coils were connected correctly. The thruster was mounted with its firing axis directed along one diagonal of the manifold tube toward one of the pumps. This was done to have a total firing length of about 4.5 m and to expand the plume in the zone where the chamber pressure was lower (Fig. 2).

Of course, to perform high-fidelity measurements of electric thrusters, vacuum-facility effects on testing must be carefully evaluated and specific test requirements must be issued. Each EP technology features its own particular physical/operational characteristics, and therefore the acceptability criteria to be adopted for test requirements differ for each particular thruster. Although some requirements already stated for low-power SPTs seem applicable for high-power models as well, a specific investigation activity should be carried out to verify this. However, this task was beyond the scope of our investigation, and we based our requirements on Fakel's past experience on high-power SPT test activities. According to that experience, a requirement of 2.8×10^{-4} torr maximum background pressure (uncorrected dynamic pressure relative to air) was assumed.

The possible enhancement of performance caused by residual background gas ingested by the Hall thruster can be estimated by means of simple gas-kinetic models.¹¹ However, because the emphasis of this work was focused on experiments and any theoretical correction can be evaluated apart, we prefer to present in this paper the original experimental data.

Before testing, the chamber background pressure was maintained for 2 h at 5×10^{-5} torr to allow the thruster to outgas. All testing was performed without opening the vacuum chamber to avoid exposing the thruster to atmosphere. No purge was used during daily facility shutdowns.

Before parametric testing and after any pause of more than 30 min, the thruster was operated for a half hour at a 300 V discharge voltage

at 3 kW to warm up the assembly. The cathode was cooled down for 25 min before each subsequent startup. Chamber venting was performed no sooner than 3 h after the last thruster shutdown to prevent oxidation of hot surfaces. The discharge voltage across electrodes, as well as rms oscillations, were measured at the vacuum tank feedthrough.

The startup sequence occurred as follows. The thruster was regulated at 300-V discharge voltage, 10-mg/s propellant mass-flow rate through the anode, and 0.55-mg/s flow rate through the cathode. The external and internal coil currents were regulated at 11 and 10.6 A, respectively. The cathode heater was supplied at 25 A for 3 min after which 300 V ignition voltage was applied on the cathode ignitor. Once the thruster was started, the currents of the external and internal magnet coils were repeatedly adjusted independently to minimize the discharge current level. Before parametric testing, the thruster was operated in this mode for a half hour to warm up the assembly. Therefore, the parametric testing was performed by selecting a nominal propellant mass-flow rate through the anode, varying in steps of 50 or 100 V the applied discharge voltage and maintaining a fixed cathode flow rate. In each selected operational mode after magnetic coils adjustment to reduce the discharge current level, the thruster was operated for at least 3 min before taking measurements. The anodic propellant mass-flow rate and the discharge voltage were increased until the power level of 12 kW was reached. The maximum discharge voltage was limited to 600 V because of the nominal operational limit of capacitors used in the electric circuit. A number of tests were repeated in order to have a good characterization of the thruster. High-voltage (600 V) and low mass-flow-rate (8 mg/s) tests were performed in a separate phase of the parametric study.

An additional test was aimed at reaching the thruster thermal equilibrium (6-kW power level) to get a number of temperature measurements to carry out a detailed thermal analysis of the thruster assembly. However, the thermal load of the plume produced an excessive heating of the vacuum chamber walls. For this reason the test was stopped before reaching thruster thermal equilibrium to avoid the risk of a failure of the vacuum gaskets with consequent damage of the facility and of the thruster. Based on results obtained in the transient state, a thermal analysis was carried out to investigate the thruster thermal status for 6- and 12-kW power levels. Figure 3 shows the calculated temperatures of the main thruster elements as a function of firing time. It is possible to see that up to 50 min of continuous operation is possible at 12 kW before the temperature of the internal coil exceeds the design requirements (400 C maximum), whereas 90 min of continuous operation is possible at a 6-kW power level. However, in both cases the pause between each firing must not be less than 8 h. A technological development and an improved version of the design is planned in order to allow for better distribution of the thermal loads.

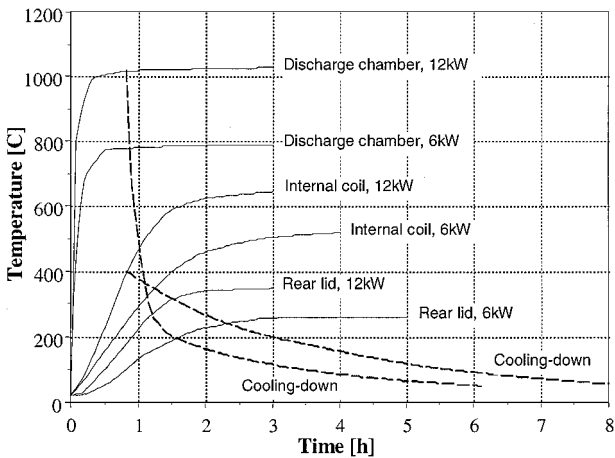


Fig. 3 Calculated temperatures of main thruster elements as a function of firing time for 6- and 12-kW operations.

Test Results and Discussion

Each startup was successful, and the thruster reached its planned operating point without problems. During the ignition, a number of sparks were observed on the insulator walls. The reason was ascribed to the presence of sputtered metallic material of the vacuum chamber on the insulator walls. Another number of sparks were observed when the engine was operated at high-voltage and low mass-flow rate (600 V, 8–10 mg/s). The cathode-neutralizer was operated at a constant mass-flow rate of 0.55 mg/s. In each operating point the engine showed steady and stable operations. The engine was characterized over a wide range of operational power levels, from 2 up to 12 kW. Facility pressure measured with ionization gauges calibrated for air never exceeded 2.8×10^{-4} torr (uncorrected value). The maximum efficiency of 0.63 at 2950 s specific impulse were obtained at the 11 kW power level. The value of the specific impulse and efficiency presented in the paper are inclusive of all power losses as well the cathode flow.

Some electrical characteristics of the thruster are presented in Fig. 4. For each mass-flow rate the current level was about constant and did not depend on the discharge voltage, meaning that the engine was operated in a regime of full acceleration. Figure 5 shows the dependency between the specific impulse and the discharge voltage

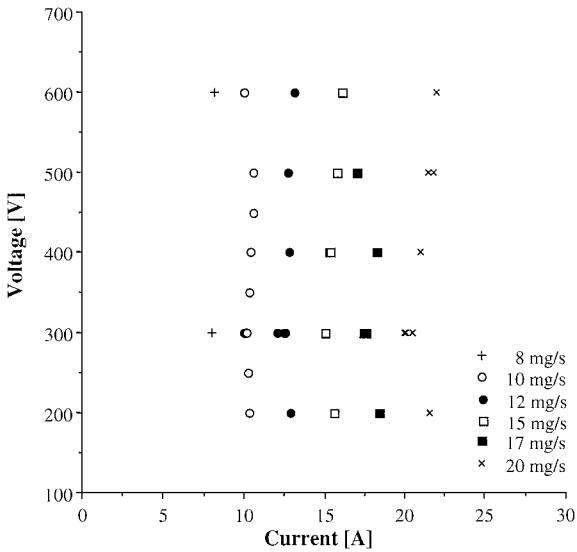


Fig. 4 Electrical characteristics for different mass-flow rates.

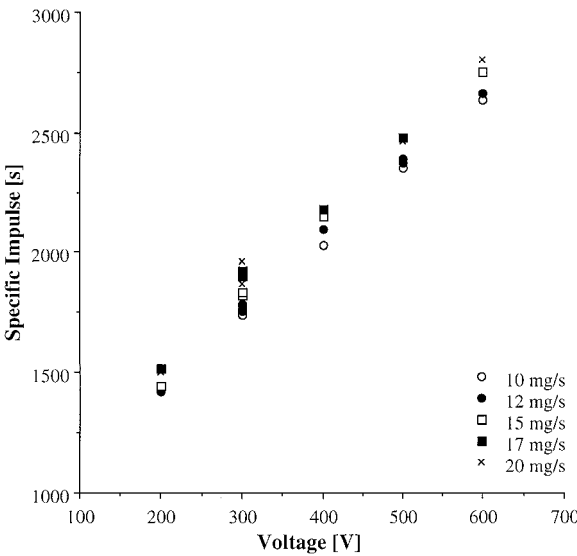


Fig. 5 Specific impulse vs discharge voltage for different mass-flow rates.

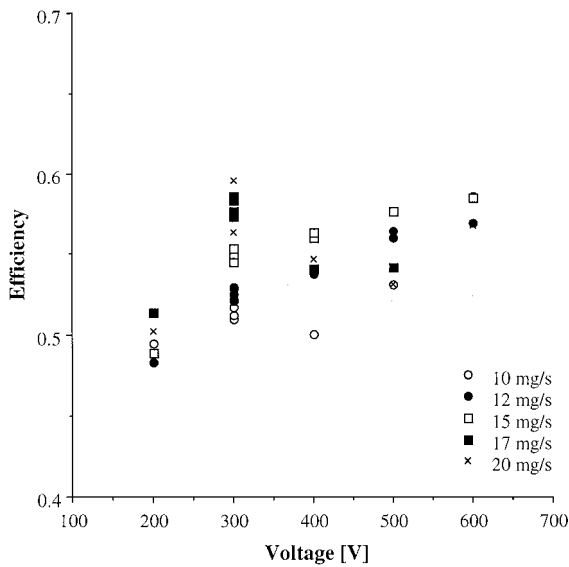


Fig. 6 Total efficiency vs discharge voltage for different mass-flow rates.

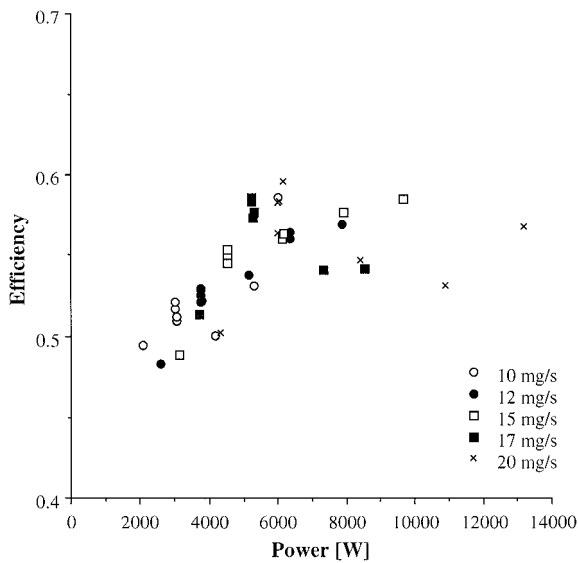


Fig. 7 Total efficiency vs discharge power for different mass-flow rates.

for different mass-flow rates. It is possible to see that at a given mass-flow rate the specific impulse varied linearly with the discharge voltage. For different mass-flow rates we have a family of parallel lines, the higher the mass-flow rate the higher the line.

The efficiency did not depend linearly on the voltage nor on the power level (Figs. 6 and 7). At any mass-flow rate the efficiency shows a relative maximum at around 300 V, a relative minimum at around 400–500 V, and then another maximum at around 500–600 V. The specific impulse was linear with the power level. However, for different mass-flow rates the lines $I_{sp} = f(\text{Power})$ have different slopes, and at a fixed power level the engine showed higher specific impulse at lower mass-flow rates (Fig. 8). In fact, the lower the mass-flow rate the lower the current and the higher the voltage.

Additional tests were performed to investigate the thruster performance at the design power level of 6 kW. The higher efficiency was obtained for 300 (1928 s specific impulse and 59% efficiency) and 600-V discharge voltage (2638 s specific impulse and 59% efficiency). At 400–500 V the efficiency decreased to 56%.

For a given mass-flow rate the trend of the ion current fraction followed the efficiency, i.e., an increase of the efficiency translated into an increase of the ion current fraction (Fig. 9) and vice versa. The highest efficiency (0.63) was obtained at the highest ion current

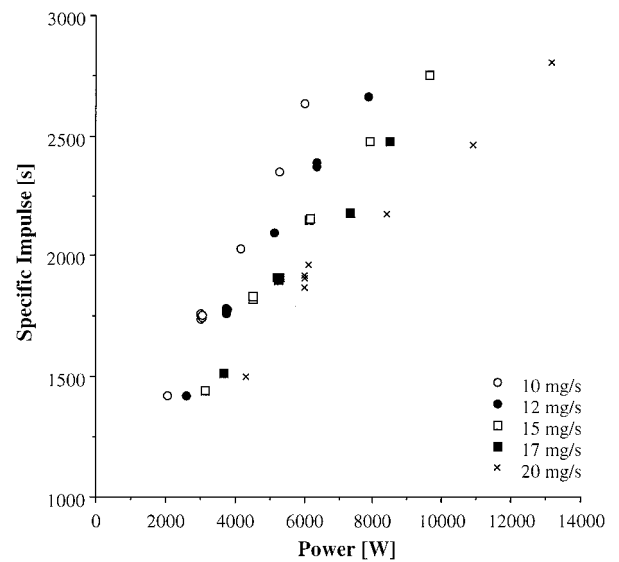


Fig. 8 Specific impulse vs discharge power for different mass-flow rates.

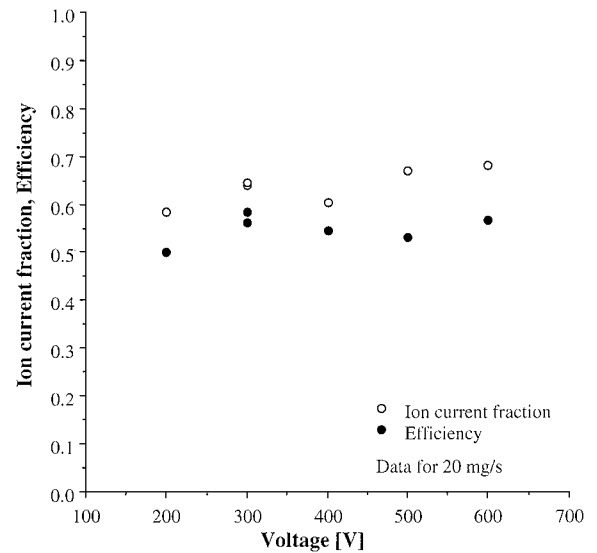


Fig. 9 Ion current fraction and total efficiency vs discharge voltage for 20 mg/s mass-flow rate.

fraction (0.72). The higher the mass-flow rate was, the higher the positive effect of a high ion current fraction. An average ion current fraction of 0.65 was measured at the 300-V discharge voltage level, resulting in a propulsive efficiency of 0.52 at 10 mg/s, 0.55 at 15 mg/s, and 0.58 at 20 mg/s.

The amplitude of current and voltage oscillations depends mainly on the voltage level. Figures 10–12 show the rms values of current and voltage oscillations measured at different voltages and mass-flow rates. At every mass-flow rate the oscillations have a remarkable increase when the thruster operates at around the 400–500-V level. This increase is higher at low mass-flow rates (10 mg/s) and at high mass-flow rates (17 and 20 mg/s). Operations at medium mass-flow rates (12 and 15 mg/s) show a rather regular behavior of oscillations; however, maximum oscillation levels were recorded at 400 V. This behavior exactly reflects the behavior of the efficiency. This fact is not surprising as the oscillations are connected to the intrinsic physical nature of the propulsive phenomenon. A further observation of the ion current measurements can shed some light on this relationship.

By observing Figs. 9–12 it is possible to see that the increase of oscillations reflects a decrease of the ion current fraction, i.e.,

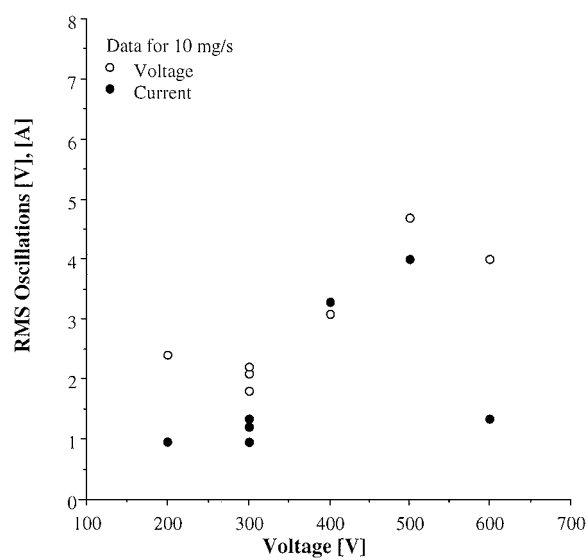


Fig. 10 Rms current and voltage oscillations vs discharge voltage for 10 mg/s mass-flow rate.

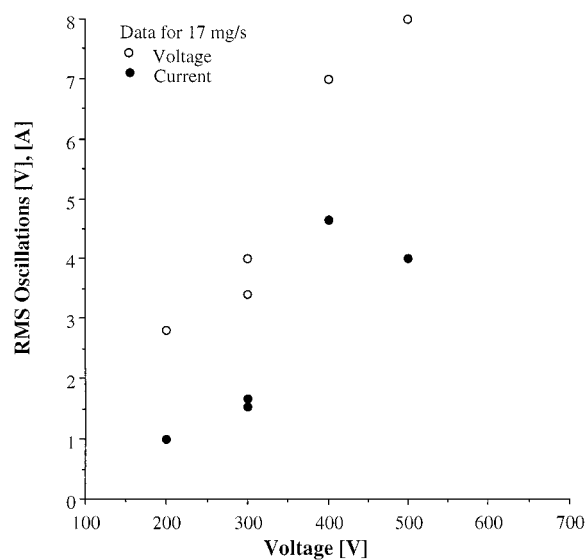


Fig. 11 Rms current and voltage oscillations vs discharge voltage for 17 mg/s mass-flow rate.

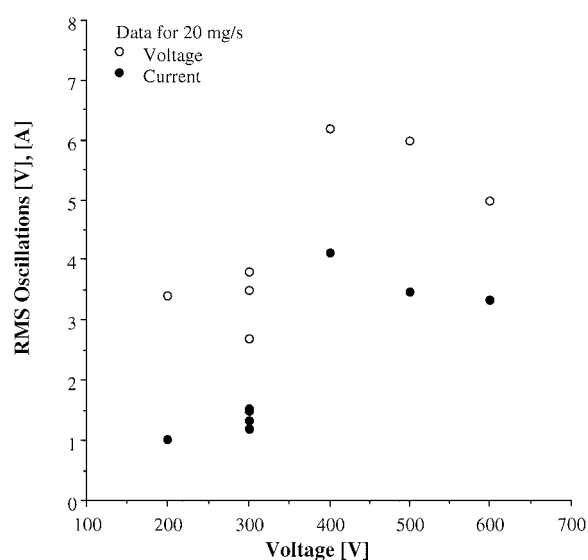


Fig. 12 Rms current and voltage oscillations vs discharge voltage for 20 mg/s mass-flow rate.

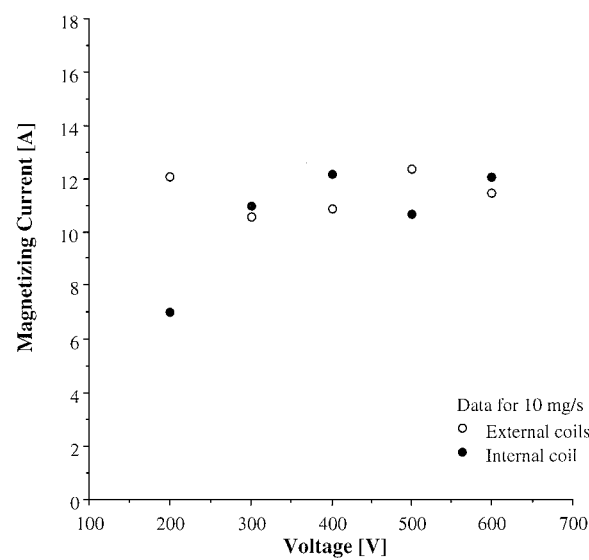


Fig. 13 Magnetizing current vs discharge voltage for 10 mg/s mass-flow rate.

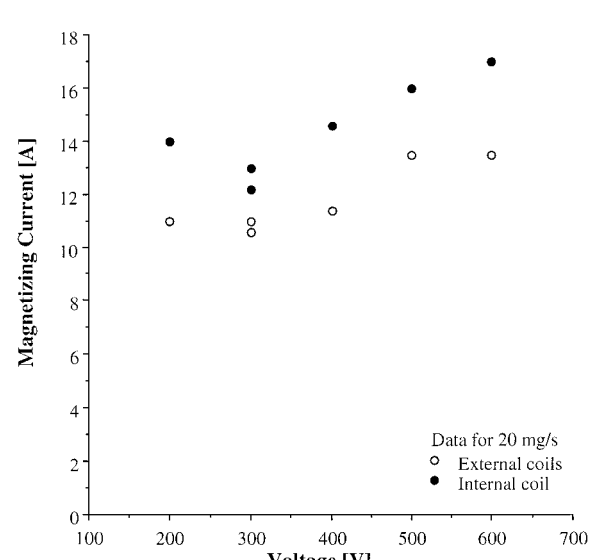


Fig. 14 Magnetizing current vs discharge voltage for 20 mg/s mass-flow rate.

the increase of oscillations leads to a decrease of the ionization efficiency. The reason for this thruster behavior can be associated both with the particular configuration of the magnetic field and of the electric filter that have been adopted for this thruster.

The level of currents in the external and internal coils was about the same. However, the internal coil presented a higher resistance than the external coil. As a result, the heat losses on the internal coil were higher. At high mass-flow rates the magnetizing currents had to be increased when the voltage level was increased. This resulted in an increase of the impedance of the discharge, as the discharge current level remained about constant. Such a trend was not visible for low mass-flow rates, however. Figures 13 and 14 show the dependency between the external and internal coil currents and the discharge voltage at 10 and 20 mg/s, respectively.

The characteristic frequency of the discharge current remained in the range of 25–30 kHz for all operational points.

The analysis of SPT-200 conditions after testing showed that all of the electrical resistances playing a major role (that of the magnetic coils, the cathode-compensator heater, the insulation between anode-cathode, anode-thruster housing, ignitor-thruster housing, cathode-thruster housing) corresponded to the requirements of the design documentation.

The visual observation of the discharge chamber conditions after tests (about 20 h in overall) showed that very little erosion took place at the exit of its external and internal walls. The length of the erosion zone near the exit of the external wall was about 8 mm, whereas on the internal wall it was about 12 mm.

Conclusions

Parametric tests on an SPT-200 thruster were carried out in the 2- to 12-kW power level range. The thruster showed good performance through the entire operational envelope. A maximum of 2950 s specific impulse and 0.63 total efficiency were obtained at 11 kW of total power. The power loss on the magnets represented about 1% of the total input power. Large oscillations were registered at 400–500 V discharge voltage, which are reflected on propulsive performance. However, total efficiencies well above 0.5 were obtained throughout.

The following areas of development were envisaged: 1) development of an upgraded mechanical construction capable of withstanding and better distributing thermal loads; 2) development of new mechanical, fluidic, and electrical interfaces designed for high power (as well as high voltage); and 3) development of an advanced configuration of the magnetic system capable of increasing the performance level and the development of a new type of heater-less cathode-compensator to be mounted axially on the thruster, inside the central pole.

Acknowledgments

The authors wish to acknowledge the precious support received by Fakel personnel. In particular, the authors would like to thank S. Muraviov for his assistance in operating the test facility and A. I. Koriakin for his assistance in the test activity.

The work described in this paper was sponsored by the International Association for the Promotion of Cooperation with Scientists from the New Independent States of the former Soviet Union (INTAS) under project 94-559 "Plasma Sources for Space Propulsion." The scientific officials who monitored the project at INTAS were J. Askeröi and Y. Beguin.

References

- ¹Bober, A. S., and Maslennikov, N. A., "SPT in Russia—New Achievements," 24th International Electric Propulsion Conf., IEPC Paper 95-6, Sept. 1995.
- ²Maslennikov, N. A., "Lifetime of the Stationary Plasma Thruster," 24th International Electric Propulsion Conf., IEPC Paper 95-75, Sept. 1995.
- ³Arhipov, B. A., Maslennikov, N. A., and Scortecci, F., "Hall Thruster Development for Primary Propulsion," Workshop on Space Basic Research and Development Cooperation Between Europe and NIS, June 1997.
- ⁴Bishaev, A., Kalashnikov, V., Kim, V., Khartov, S., Shavykina, A., and Scortecci, F., "The Simulation of the Sputtered Particle Dynamics in the SPT Plume," *Proceedings of the 2nd European Spacecraft Propulsion Conference*, ESA-SP-398, Noordwijk, The Netherlands, 1997, pp. 349–353.
- ⁵Bishaev, A., Kalashnikov, V., Khartov, S., Kim, V., Kozlov, V., and Popov, G., "Theoretical and Experimental Studies of Low Pressure Discharge with Closed Hall Current," International Association for Promotion of Cooperation with Scientists from the New Independent States of Former Soviet Union, INTAS Project 94-559, TR, Moscow, May 1996.
- ⁶Arhipov, B. A., Maslennikov, N. A., and Scortecci, F., "Experimental Investigation of SPT-200 Performance and Operational Characteristics," International Association for Promotion of Cooperation with Scientists from the New Independent States of Former Soviet Union, INTAS Project 94-559, TR, Moscow, Aug. 1996.
- ⁷Morozov, A. I., Esipchuk, Y. V., Tilinin, G. N., Trofimov, A. V., Sharov, Y. A., and Shchepkin, G. Y., "Plasma Accelerator with Closed Electron Drift and Extended Acceleration Zone," *Soviet Physics-Technical Physics*, Vol. 17, No. 1, 1972, pp. 38–45.
- ⁸Bugrova, A. I., Kim, V. P., Maslennikov, N. A., and Morozov, A. I., "Physical Processes and Characteristics of Stationary Plasma Thrusters with Closed Electrons Drift," 22nd International Electric Propulsion Conf., IEPC Paper 91-79, Oct. 1991.
- ⁹Gavryushin, V. M., Kim, V. P., and Maslennikov, N. A., "Physical and Technical Bases of the Modern SPT Development," 24th International Electric Propulsion Conf., IEPC Paper 95-38, Sept. 1995.
- ¹⁰Arhipov, B. A., Gnizdor, R., Kozubsky, K. N., Maslennikov, N. A., Kim, V. P., Day, M., Randolph, T. M., and Rogers, W. P., "SPT-100 Module Lifetime Test Results," AIAA Paper 94-2854, June 1994.
- ¹¹Garner, C. E., Tverdokhlebov, S. O., Seminkin, A. V., and Garkusha, V. I., "Evaluation of a 4.5-kW D-100 Thruster with Anode Layer," AIAA Paper 96-2967, July 1996.